2013 10th IEEE International Conference on Control and Automation (ICCA)
Hangzhou, China, June 12-14, 2013

Optimal Preview Control of Dual-Stage Actuators System for Triangular Reference Tracking*

Li Wang[1], Jinchuan Zheng[2], and Minyue Fu[3]

Abstract— **This paper proposes an optimal preview control law for a dual-stage actuators (DSA) system to track triangular references, which is essential in many raster scan motion control applications. The main difficulty of tracking triangular reference is to follow the waveform fast and accurately when its slope switches. For this goal, we first present a non-preview time optimal control for the primary stage, which is proved to have the minimal overshoot. This result is a new contribution to DSA control because it leads to a minimal reference profile for secondary stage to follow and thus significantly prevents the saturation of the secondary actuator. Next, we propose an optimal preview control with the use of the information of the future references to further reduce the settling time and the overshoot. Finally, the secondary actuator controller is also given. Simulated results are shown to verify the effectiveness of the proposed control design.**

I. INTRODUCTION

Dual-stage actuators (DSA) servomechanisms are typically characterized by a structural design with two actuators connected in series along a common axis. The primary actuator (coarse actuator) is of long travel range but with poor accuracy and slow response. The secondary actuator (fine actuator) is typical of higher precision and faster response but with a limited travel range. By combining the DSA system with properly designed servo controllers, the two actuators are complementary to each other and the defects of one actuator can be compensated by the merits of the other one. Therefore, the DSA system can provide large travel range, high positioning accuracy and fast response. The DSA servomechanisms have attracted considerable industrial application such as the dual-stage hard disk drive actuator [1], [2], the dual-stage machine tools [3], macro/micro robot manipulators [4], and dual-stage positioning tables [5], [6].

The mechanical design of DSA systems appears to be simple, but the control of the DSA systems is not straightforward because of several reasons. Firstly, the DSA systems contains two control inputs but only one control output, which requires proper control strategy for control allocations of the two actuators in response to a reference input. Secondly, the actuators have input constraints in practice, which results in difficulties when actuator saturation occurs. As such, these specific characteristics have raised challenging tasks for DSA control design to yield an optimal performance. A variety of approaches have been reported to deal with the dual-stage control problems. For example, the control design for track following and settling (i.e, disturbance and residual vibration rejection control problem) can be found in [7]. The secondary actuator saturation problem was explicitly taken into account during the control design [8]–[10]. Tracking control is another main control task to drive the position output to track a desired trajectory such as setpoint references which is used to perform pick-and-place operations in nanoassembly [11] and power sintering process [12]. Moreover, triangular reference is the most common trajectories used in scanning probe devices, which typical combine a triangular waveform in the X-axis and a linear ramp in the Y-axis to achieve the desired raster scan motion [13], [14]. Though the setpoint tracking control has been extensively discussed [15], [16], triangular reference tracking control is rarely studied in the literature. Therefore, this paper is focused on the control of DSA systems for triangular reference tracking with fast and accurate performance.

Because of the redundancy of actuators, the dual-stage control design is divided into two control problems, one for each stage. The primary stage control problem is to enable the primary actuator to track the triangular reference in minimal time when the slope changes, whilst allowing the tracking error within a manifold, which thus motivates the preview control. The secondary-stage control problem is then to make the secondary actuator to compensate for the tracking error produced by the primary actuator, which if achieved can lead to tracking the triangular reference accurately.

Our contribution in this paper is the proposed new optimal preview control for the primary actuator. In particular, we develop a non-preview time optimal controller and an optimal preview controller. It is proved that these controllers have the properties of both time optimal and minimal tracking error performance. Our preview control differs from the conventional preview control [17], which uses the augmented system with the preview information to generate the preview feedforward control input that may require a large computational load. In our work, we give the optimal control directly for the continuous time system and the result has a simple explicit expression without solving a complex optimization problem. Another advantage of our work is that we give an explicit expression for the required preview time. For the secondary actuator control design, we simple employ a nonlinear feedback controller. As such, the combined dual-

* This work was supported by the NSFC under Grant 61134001.

[1]L. Wang is with the School of Control Science and Engineering, Zhejiang University, Hangzhou, China. li.wangzju@gmail.com

[2]J. Zheng is with the Faculty of Engineering and Industrial Sciences, Swinburne University of Technology, Hawthorn, VIC 3122, Australia. jzheng@swin.edu.au

[3]M. Fu is with the School of Electrical Engineering and Computer Science, University of Newcastle, NSW 2308 Australia. He also holds a Qian-ren Professorship at Zhejiang University, China. minyue.fu@newcastle.edu.au

stage controller is shown to achieve fast and accurate tracking of triangular references as verified by simulated results.

The rest of this paper is organized as follows. Section II presents the DSA model and formulates the dual-stage control problems. Section III derives the solution for the primary-stage control which includes a non-preview controller and a preview controller. Section IV simply gives the controller design for the secondary actuator. Section V shows the simulation results of the proposed control to validate its effectiveness. Finally, concluded remarks and future work are given in Section VI.

II. PROBLEM FORMULATION

We consider a class of DSA system that can be depicted by Fig. 1, where M and m denote the mass of the primary and secondary stage, respectively, F_1 and F_2 the actuator applied control force, and y the total position output of the DSA. During the process of mechanism design, it is typical to select the configurations of two stages such that $M \gg m$, $|y_1| \gg |y_2|$, and $|F_2/F_1| \gg m/M$. In this way, the coupling forces between the two actuators can be simply ignored and the dynamic equations of the DSA system are given by:

$$\begin{cases} M\ddot{y}_1 = F_1. \\ m\ddot{y}_2 = F_2 - c_0\dot{y}_2 - k_0 y_2. \end{cases} \tag{1}$$

A typical experimental setup that matches the model in Fig. 1 has been developed [16], where the primary stage is driven by a linear motor and the secondary stage by a piezoelectric actuator. Suppose the power amplifier gain of each actuator is g_1 and g_2, respectively and substitute $F_i = g_i u_i$ $(i = 1, 2)$ to (1), where u_i is the actuator control input. We can easily obtain the state-space model for the DSA system as follows:

$$\begin{cases} \Sigma_1 : \dot{x}_1 = A_1 x_1 + B_1 u_1 \\ \Sigma_2 : \dot{x}_2 = A_2 x_2 + B_2 u_2 \\ \qquad y = y_1 + y_2 = C_1 x_1 + C_2 x_2 \end{cases} \tag{2}$$

where the state $x_1 = [y_1 \;\; \dot{y}_1]^T$, $x_2 = [y_2 \;\; \dot{y}_2]^T$, and

$$A_1 = \begin{bmatrix} 0 & 1 \\ 0 & 0 \end{bmatrix}, B_1 = \begin{bmatrix} 0 \\ b_1 \end{bmatrix}, C_1 = \begin{bmatrix} 1 \, 0 \end{bmatrix},$$

$$A_2 = \begin{bmatrix} 0 & 1 \\ a_1 & a_2 \end{bmatrix}, B_2 = \begin{bmatrix} 0 \\ b_2 \end{bmatrix}, C_2 = \begin{bmatrix} 1 \, 0 \end{bmatrix}.$$

with $b_1 = \frac{g_1}{M}$, $a_1 = -\frac{k_0}{m}$, $a_2 = -\frac{c_0}{m}$ and $b_2 = \frac{g_2}{m}$. Moreover, the control inputs of the two actuators and the secondary actuator output have the constraints:

$$|u_1| \le \bar{u}_1, \;\; |u_2| \le \bar{u}_2, \;\; |y_2| \le \bar{y}_2. \tag{3}$$

where $\bar{u}_1$ and $\bar{u}_2$ denote the maximum control input of the actuator, respectively, and $\bar{y}_2$ is the maximum travel range of the secondary actuator.

For the DSA system in (2), our control aim is to design the control law u_1 and u_2 such that the total DSA output can accurately track a triangular reference $r(t)$ with a frequency as high as possible, where $r(t)$ is shown in Fig.2. An intuitive

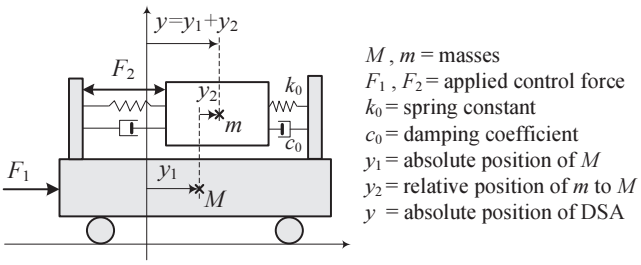

Fig. 1. Illustration of a class of DSA model

control strategy is to design u_1 to track the reference at its best capability and then u_2 is designed to follow the residual tracking error of the primary actuator. Provided that the tracking error is within the secondary actuator's travel range and the secondary actuator has a much faster dynamics, the resulting total tracking error of the DSA will be negligible. In general, the control difficulty occurs when the slope of the triangular reference changes because the primary stage typically suffers from an overshoot and requests a tedious time to settle down to steady state. Therefore, in the sequel we will focus on how to design u_1 to reduce the transition time and the overshoot. Moreover, we propose a preview control method if the further information of the reference is known in advance. Fig. 2 illustrates the preview control strategy. We assume that the period of the reference is sufficiently long so that the tracking error will be able to reach zero before the waveform switches direction. Furthermore, we have the following definitions:

1) The tracking error of the primary stage is denoted by:
$$e_1(t) = y_1(t) - r(t) \tag{4}$$
2) The overshoot denotes the maximum tracking error:
$$\text{overshoot} = \max |e_1(t)| \tag{5}$$
3) The minimum overshoot is denoted by σ, which is defined by:
$$\sigma = \min_{u_1 \in \mathcal{U}} \max |e_1(t)| \tag{6}$$
where $\mathcal{U}$ represents the set of all feasible control inputs.

Hence, the DSA control problems is formulated as follows:

A. Primary Actuator Control Problem

For a given triangular reference $r(t)$, find a controller:

$$u_1(t) = \begin{cases} u_{1-}(t), & -\tau_p \le t \le 0 \\ u_{1+}(t), & t > 0 \end{cases} \tag{7}$$

subject to:

$$|u_1(t)| \le \bar{u}_1 \tag{8}$$

and an appropriate preview time $\tau_p \ge 0$ such that:

$$\sigma \text{ is achieved.} \tag{9}$$

Based on the (9), there are two other goals:

$$\tau_s \text{ is minimized.} \tag{10}$$

$$\tau_p \text{ is minimized.} \tag{11}$$

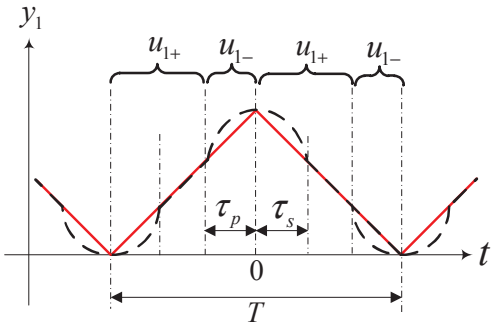

Fig. 2. Illustration of preview control strategy for the primary actuator. The solid line denotes the triangular reference $r(t)$ and the dashed line the output response of the primary actuator $y_1(t)$ with pre-actuation. We set the time $t = 0$ to represent the switching time instant at which the slope of the triangular reference switches; τ_p the preview time; τ_s the settling time; and T the period of the triangular reference. u_{1-} represents the preview control input and u_{1+} the post-actuation control input; and the brackets underneath represent the time zones that the control inputs apply to.

If such an u_1 exists, we call it an optimal preview control. Moreover, if we choose $\tau_p = 0$, then the resulting controller is called non-preview time-optimal control.

B. Secondary Actuator Control Problem

Given the designed primary actuator controller, find a controller:

$$|u_2(t)| \le \bar{u}_2 \tag{12}$$

such that the secondary actuator output y_2 can compensate for the tracking error generated by the primary actuator, i.e, $y_2 \approx -e_1$. As a result, we can achieve:

$$y = y_1 + y_2 = e_1 + r + y_2 \approx r \tag{13}$$

which implies that the total DSA output can track the triangular reference accurately.

III. PRIMARY ACTUATOR CONTROL DESIGN

This section addresses the solution to the primary actuator control problem as stated in Sec. II-A. We first derives a time-optimal control (TOC) law without preview, based upon which an optimal preview control law is proposed. Finally, a PTOS controller is combined with the proposed control law to achieve robust tracking performance.

A. Non-Preview Time-Optimal Control

We first transform the primary actuator system into the error space with the following form:

$$\dot{x}_e = \begin{bmatrix} 0 & 1 \\ 0 & 0 \end{bmatrix} x_e + \begin{bmatrix} 0 \\ b_1 \end{bmatrix} u_1 \tag{14}$$

where $x_e = [e_1 \quad \dot{e}_1]^T$, $|u_1| \le \bar{u}_1$, and the initial state of the system is given by:

$$x_e(0) = [e_1(0) \quad \dot{e}_1(0)]^T \tag{15}$$

Firstly, we aim to find a time-optimal controller $u_1(t)$, $t \ge 0$ for the system (14) to achieve the goals of (10) for any initial state $x_e(0)$. It is well-known that the solution is a bang-bang function [18], whose control law is directly given by:

$$u_1^*(t) = \text{sign}^\dagger\big(-\text{sign}(e_1(t))\sqrt{2b_1\bar{u}_1|e_1(t)|} - \dot{e}_1(t), e_1(t)\big)\bar{u}_1 \tag{16}$$

where sign$(\cdot)$ and sign$^\dagger(\cdot\ ,\cdot)$ are defined as follows:

$$\text{sign}(\Omega) = \begin{cases} +1, & \Omega > 0 \\ -1, & \Omega < 0 \\ 0, & \Omega = 0 \end{cases} \tag{17}$$

$$\text{sign}^\dagger(\Omega_1, \Omega_2) = \begin{cases} \text{sign}(\Omega_1), & \Omega_1 \ne 0 \\ \text{sign}(\Omega_2), & \Omega_1 = 0 \end{cases} \tag{18}$$

Next, we address a very useful property of the control law above.

Lemma 3.1: The time-optimal control law u_1^* (16) for the system (14) is also the optimal control law for the minimum overshoot σ as defined by (6), i.e., the goal (9) is also achieved under the same control law. Furthermore, the minimum overshoot equals to:

$$\sigma = \max\big(|e_1(0)|, |e_1(0) + \frac{\dot{e}_1(0)|\dot{e}_1(0)|}{2b_1\bar{u}_1}|\big) \tag{19}$$

Proof: According to the locations of the initial state in phase plane as shown in Fig. 3, we divide the right-half plane into three regions indicated by I, II, and III, where the curve going through the point $O(0,0)$ is:

$$\dot{e}_1(t) = -\text{sign}(e_1(t))\sqrt{2b_1\bar{u}_1|e_1(t)|} \tag{20}$$

For the initial states in the left-half plane, it is easy to follow the similar divisions and proof procedure as stated below, which are omitted for simplicity.

Suppose each region contains a sample point A, B, and C, respectively. Applying the time-optimal control law u_1^* (16) to the system (14), it is straightforward to verify that the state trajectory of $(e_1(t), \dot{e}_1(t))$ is parabola, which appears as the three cases of curves as shown in Fig. 3. The curves going upwards correspond to $u_1 = \bar{u}_1$, and those going downwards correspond to $u_1 = -\bar{u}_1$. The point $O(0,0)$, which is the target state, corresponds to $u_1 = 0$.

To prove the time-optimal control law $u_1^*(t)$ can also achieve the minimum overshoot compared with other control law, we define $(e_1^*(t), \dot{e}_1^*(t))$ as the state response under u_1^*, while $(e_1(t), \dot{e}_1(t))$ under non-optimal control law $|u(t)| \le \bar{u}_1$. In the sequel, we derive the result (19) by proving three cases as follows:

Case 1: When the initial state $x_e(0)$ is in region I, e.g., point $A(e_1(0), \dot{e}_1(0))$ (see Fig. 3), then the state trajectory under u_1^* starts with $u_1 = -\bar{u}_1$ until getting to point A'' and then reaching the target point O by switching $u_1 = \bar{u}_1$. It can be easily seen from Fig. 3 that the overshoot occurs at point $A'(e_1^*(t_1), 0)$, where t_1 denotes the time it takes to travel from point A to A'. Next, we consider the system is under non-optimal control law $u_1(t)$ within the time interval $t \in [0, t_1]$. Then, we have:

$$\begin{cases} \dot{e}_1^*(t) = \dot{e}_1(0) + \int_0^t b_1(-\bar{u}_1)dt & t \in [0, t_1] \\ \dot{e}_1(t) = \dot{e}_1(0) + \int_0^t b_1 u_1(t)dt & t \in [0, t_1] \end{cases} \tag{21}$$

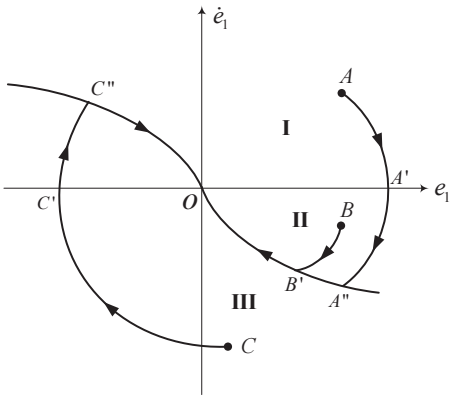

Fig. 3. System state trajectory under the time-optimal control law, which is shown to be optimal control law for minimal overshoot as well.

From the above equation, we can obtain:

$$\begin{aligned} e_1^*(t) - e_1(t) &= \int_0^t (\dot{e}_1^*(t) - \dot{e}_1(t))dt \\ &= -\int_0^t b_1(u_1(t) + \bar{u}_1)dt \\ &\le 0 \qquad\qquad t \in [0, t_1] \end{aligned} \tag{22}$$

Therefore, This implies that the time-optimal control law u_1^* has the minimal overshoot σ, which equals to:

$$\sigma = e_1^*(t_1) = e_1(0) + \frac{\dot{e}_1(0)|\dot{e}_1(0)|}{2b_1\bar{u}_1} \qquad t_1 = \frac{\dot{e}_1(0)}{b_1\bar{u}_1} \tag{23}$$

Case 2: When the initial state $x_e(0)$ is in region II, e.g., point $B(e_1(0), \dot{e}_1(0))$, then the state trajectory under u_1^* follows the curve $B \to B' \to O$. It can be easily seen from Fig. 3 that the overshoot occurs at point B and thus equals to $e_1(0)$. For non-optimal control law $u_1(t)$, we can simply get:

$$e_1^*(t) \le \sigma = e_1(0) \le \min_{u_1 \in \mathcal{U}} \max_{t \ge 0} |e_1(t)| \tag{24}$$

Case 3: When the initial state $x_e(0)$ is in region III, e.g., point $C(e_1(0), \dot{e}_1(0))$, then the state trajectory under u_1^* follows the curve $C \to C' \to C'' \to O$, where point $C'(e_1^*(t_1), 0)$ locates on X-axis. Then we have:

$$e_1^*(t_1) \le e_1^*(t) \le e_1(0) \qquad t \in [0, +\infty] \tag{25}$$

For non-optimal control law $u_1(t)$, we have:

$$e_1^*(t) - e_1(t) \ge 0 \qquad t \in [0, t_1] \tag{26}$$

It follows that:

$$e_1(t_1) \le e_1^*(t_1) \le e_1^*(t) \le e_1(0) \qquad t \in [0, +\infty] \tag{27}$$

Therefore, we have:

$$\begin{aligned} \sigma &= \max\left(|e_1(0)|, |e_1^*(t_1)|\right) \\ &= \max\left(|e_1(0)|, |e_1(0) + \frac{\dot{e}_1(0)|\dot{e}_1(0)|}{2b_1\bar{u}_1}|\right) \end{aligned} \tag{28}$$

We can easily follow the above procedure to get the results for initial states in left-hand plane. Combined the results from the different cases, we can finally get the result in (19). Then the proof is completed. □

Remark 3.1: We know that using TOC $u_1^*(t)$ to drive the primary actuator from $x_e(t_2) = [p, -v]$ to $x_e(t_2 + t_r) = 0$ will produce the minimum overshoot σ. The process can be inversed, we can drive the primary actuator from $x_e(t_1) = 0$ to $x_e(t_1 + t_r) = [p, v]$ by applying TOC $u^*(t)$. Either tracking error trajectory is the mirroring of the other. So:

$$\begin{aligned} \min_{u_1 \in \mathcal{U}} \max_{t_1 \le t \le t_1 + t_r} |e(t)| &= \min_{u_1 \in \mathcal{U}} \max_{t_2 \le t \le t_2 + t_r} |e(t)| \\ &= \max(|p|, |p - \frac{v|v|}{2b_1\bar{u}_1}|) \end{aligned} \tag{29}$$

B. Optimal Preview Control

The preview control algorithm takes the advantage of the information of the triangular reference to further reduce the overshoot. The optimal preview controller can achieve the goals (9)-(11) stated as follow:

Lemma 3.2: The preview controller $u_{1-}(t)$ with the following form:

$$u_{1-}(t) = \begin{cases} \text{sign}(v_1 - v_2)\bar{u}_1, \\ \quad -\frac{|v_1 - v_2|}{b_1\bar{u}_1} \le t \le -\frac{3|v_1 - v_2|}{4b_1\bar{u}_1} \\ -\text{sign}(v_1 - v_2)\bar{u}_1, \\ \quad -\frac{3|v_1 - v_2|}{4b_1\bar{u}_1} < t \le 0 \end{cases} \tag{30}$$

can lead to the minimal overshoot:

$$\sigma = \frac{|v_1 - v_2|^2}{16b_1\bar{u}_1} \tag{31}$$

where $v_1 = \dot{r}(t)$, $t \in (-\infty, 0)$ and $v_2 = \dot{r}(t)$, $t \in (0, \infty)$.

Proof: Because the primary actuator output trajectory and velocity is continuous so that:

$$\begin{cases} e_1(0^-) = e_1(0^+) = e_1(0) \\ \dot{e}_1(0^-) = \dot{y}_1(0) - v_1 \\ \dot{e}_1(0^+) = \dot{y}_1(0) - v_2 \end{cases} \tag{32}$$

When $-\tau_p \le t \le 0$, from *Remark 3.1*, we can get:

$$\sigma_1 = \max(|e_1(0)|, |e_1(0) - \frac{\dot{e}_1(0^-)|\dot{e}(_1 0^-)|}{2b_1\bar{u}_1}|) \tag{33}$$

And when $t > 0$, from *Lemma3.1*, we can get:

$$\sigma_2 = \max(|e_1(0)|, |e_1(0) + \frac{\dot{e}_1(0^+)|\dot{e}_1(0^+)|}{2b_1\bar{u}_1}|) \tag{34}$$

Hence, we have:

$$\begin{aligned} \sigma &= \max(\sigma_1, \sigma_2) \\ &= \max(|e_1(0)|, |e_1(0) - \frac{(\dot{y}_1(0) - v_1)|\dot{y}_1(0) - v_1|}{2b_1\bar{u}_1}|, \\ &\quad |e_1(0) + \frac{(\dot{y}_1(0) - v_2)|\dot{y}_1(0) - v_2|}{2b_1\bar{u}_1}|) \end{aligned} \tag{35}$$

Moreover, $\sigma = \frac{|v_1 - v_2|^2}{16b_1\bar{u}_1}$ only when $e_1(0) = -\text{sign}(v_1 - v_2)\frac{|v_1 - v_2|^2}{16b_1\bar{u}_1}$ and $\dot{y}(0) = \frac{v_1 + v_2}{2}$. We can calculate the TOC control signal $u_{1-}(t)$ which drive the primary stage from $x_e(-\tau_p) = 0$ to $x_e(0^-) = [-\text{sign}(v_1 - v_2)\frac{|v_1 - v_2|^2}{16b_1\bar{u}_1}, \frac{v_2 - v_1}{2}]$ by the optimal time theory. The $u_{1-}(t)$ is shown in (30).

Thus, the proof is completed. □

Remark 3.2: Consider a special case with $v_1 = -v_2 = v$,

according to (31), we can obtain:

$$\sigma = \frac{v^2}{4b_1\bar{u}_1} \tag{36}$$

under optimal preview control. Compared with the result without preview (19) where we will set $e_1(0) = 0$ and $\dot{e}_1(0) = 2v$ for a fair comparison, then we can obtain:

$$\sigma = \frac{2v^2}{b_1\bar{u}_1} \tag{37}$$

Obviously, the optimal preview control has greatly reduced the overshoot by 8 times.

C. Combination with PTOS for Practical Implementation

For practical implementation and robustness, the proximate time-optimal servomechanism (PTOS) [18] is typically incorprated into time-optimal control. Its control law is given below:

$$u_{1+} = \text{sat}[k_2(-f(e_1) - \dot{y}_1 + \dot{r})] \tag{38}$$

where

$$f(e_1) = \begin{cases} \frac{k_1}{k_2}e_1 & |e_1| \le y_l \\ \text{sign}(e_1)\left(\sqrt{2b_1\bar{u}_1|e_1|} - \frac{\bar{u}_1}{k_2}\right) & |e_1| > y_l \end{cases} \tag{39}$$

where sat[$\cdot$] is with the saturation level of $\bar{u}_1$, k_1 and k_2 are constant gains which can be designed by traditional pole-placement method [18]. $\dot{r}(t)$ is the derivative of $r(t)$ with the convention that $\dot{r}(0) = 0$ when slope changes. The following constraints guarantee a continuous switching of the controller:

$$y_l = \frac{\bar{u}_1}{k_1}, \quad k_2 = \sqrt{\frac{2k_1}{b_1}}. \tag{40}$$

where y_l is the linear region close to the setpoint which is introduced to reduce the control chatter.

IV. SECONDARY ACTUATOR CONTROL DESIGN

The secondary actuator controller is a composite nonlinear feedback controller [16]. Its control law is given by:

$$u_2 = u_{2L} + u_{2N}, \tag{41}$$

where u_{2L} is a linear feedback control law and:

$$u_{2L} = Wx_2, \tag{42}$$

where $W = [w_1 \quad w_2]$ can be calculated by linear control design methods to achieve a higher bandwidth.

The nonlinear feedback controller is given by:

$$u_{2N} = \phi(y, r)H \begin{bmatrix} y_1 - r \\ \dot{y}_1 - \dot{r} \end{bmatrix} \tag{43}$$

where H is given by:

$$H = \frac{1}{b_2}[(a_1 + b_2w_1 + b_1k_1) \quad (a_2 + b_2w_2 + b_1k_2)] \tag{44}$$

with constants k_1 and k_2 from the design of primary actuator, and the nonlinear function $\phi(y, r)$ is given by:

$$\phi(y, r) = e^{-\beta|y-r|} \tag{45}$$

where β is a positive parameter that can be tuned to make the DSA achieve better performance.

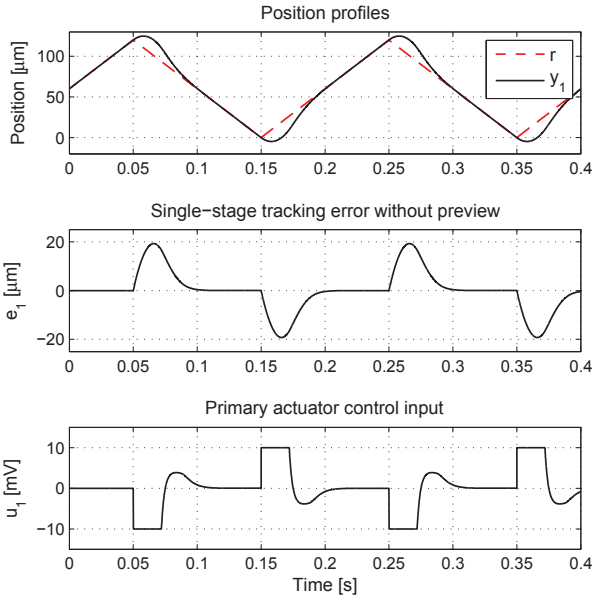

Fig. 4. Single-stage (with primary actuator only) tracking control without preview. The maximum tracking error is 20 μm.

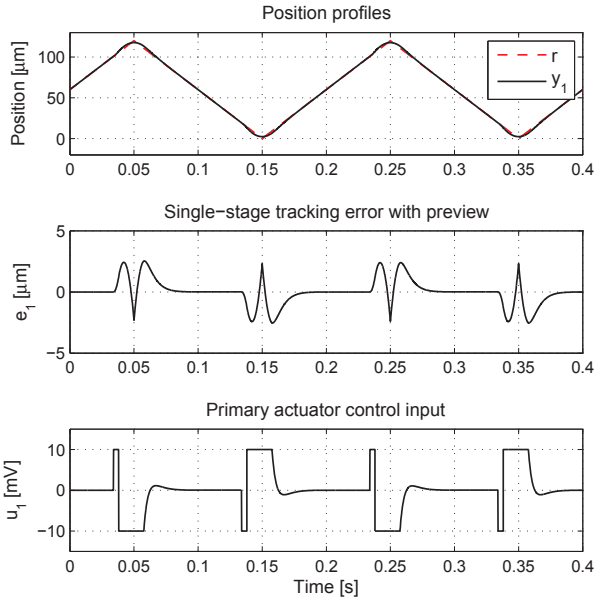

Fig. 5. Single-stage tracking control with preview. The maximum tracking error is significantly reduced to 2.4 μm due to the preview control.

V. SIMULATION RESULTS

This section presents the simulations. The triangular reference is set with the period $T = 0.2$ s and $Amplitude = 120$ μm. We assume that the states x_1 and x_2 are all measurable. The DSA model parameters in (2) are given as follows:

$$b_1 = 1.5 \times 10^7, \; b_2 = 3 \times 10^6,$$
$$a_1 = -10^6, \; a_2 = -1810,$$
$$\bar{u}_1 = 10 \text{ mV}, \bar{u}_2 = 5 \text{ V}, \; \bar{y}_2 = 15 \; \mu\text{m}.$$

Fig. 4 shows the single-stage tracking control results with the primary actuator only. The maximum tracking error is 20 μm. While the maximum tracking error is greatly reduced to 2.5 μm with preview control as shown in Fig. 5. This

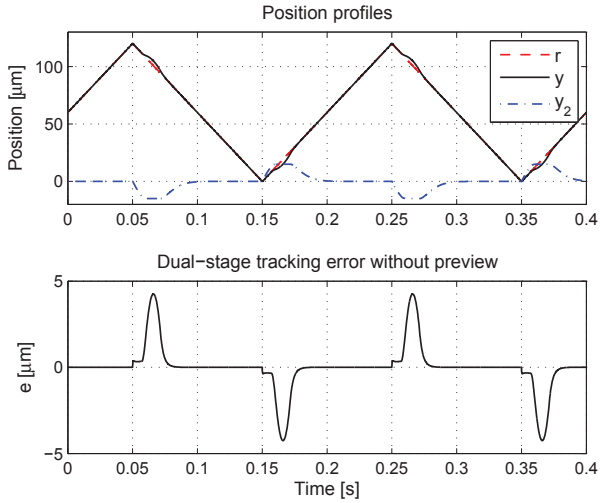

Fig. 6. Dual-stage tracking without preview control. The maximum tracking error with the use of the secondary actuator is 4.3 μm but cannot be further reduced because the maximum tracking error generated by the primary actuator without preview control is beyond the travel range of the secondary actuator as shown in Fig. 4.

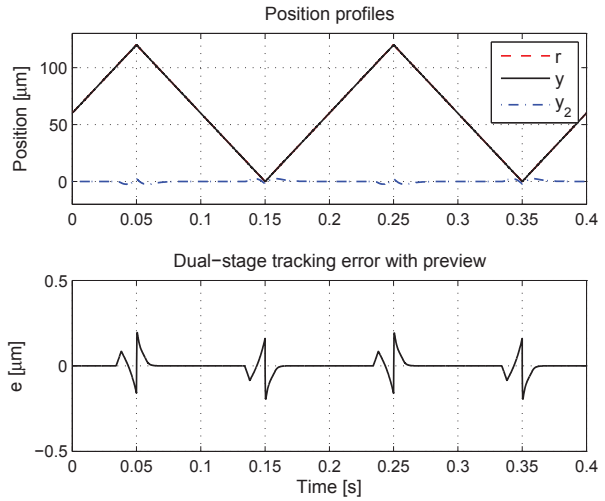

Fig. 7. Dual-stage tracking with preview control. The maximum tracking error is perfectly reduced to 0.2 μm with the preview control for the primary actuator. Moreover, the settling time is reduced to 0.016 s as compared with the case of 0.036 s without preview (see Fig. 6).

verifies the effectiveness of the proposed preview controller for reduction of the maximum tracking error. Next, we apply the optimal preview controller to the DSA system. Fig. 6 shows that the maximum tracking error achieved by the DSA without preview is 4.3 μm, which, however, cannot be further reduced because the primary actuator tracking error is beyond the travel range of the secondary actuator as shown in Fig. 4. Finally, Fig. 7 shows the maximum tracking error is significantly reduced to 0.2 μm with preview control. Moreover, the settling time achieved is only 0.018 s, which is much smaller than the case of 0.036 s without preview as shown in Fig. 6. These results coincide with our theoretical analysis. Hence, the simulation results confirm that the proposed preview controller can achieve very accurate tracking with minimal settling time but also minimal overshoot for the DSA system.

VI. CONCLUSION

In this paper, we have proposed an optimal preview control law for a DSA system to track triangular references fast and accurately. It is proved that the optimal preview control can not only reduce the settling time but also minimize the overshoot. Simulated results are shown to verify the effectiveness of the proposed control design. Our future work will implement the proposed controller on a real DSA experimental setup and verify the control law. Implementation issues such as robustness with respect to references of different amplitudes and periods with be further investigated.

REFERENCES

[1] K. Mori, T. Munemoto, H. Otsuki, Y. Yamaguchi, and K. Akagi, "A dual-stage magnetic disk drive actuator using a piezoelectric device for a high track density," *IEEE Trans. Magn.*, vol. 27, no. 6, pp. 5298-5300, Nov. 1991.

[2] R. B. Evans, J. S. Griesbach, and W. C. Messner, "Piezoelectric microactuator for dual stage control," *IEEE Trans. Magn.*, vol. 35, no. 2, pp. 977-982, Mar. 1999.

[3] B.-S Kim, J. Li, and T.-S Tsao, "Two-parameter robust repetitive control with application to a novel dual-stage actuator for noncircular machining," *IEEE/ASME Trans. Mechatron.*, vol. 9, no. 4, pp. 644-652, Dec. 2004.

[4] S. J. Kwon, W. K. Chung, and Y. Youm, "On the coarse/fine dual-stage manipulators with robust perturbation compensator," in *Proc. IEEE Int. Conf. Robotics and Automation*, 2001, pp. 121-126.

[5] A. T. Elfizy, G. M. Bone, and M. A. Elbestawi, "Design and control of a dual-stage feed drive," *Int. Journal of Machine Tools & Manufacture*, vol. 45, pp. 153-165, 2005.

[6] J. Zheng, A. Salton, and M. Fu, "Design and control of a dual-stage actuator positioning system," *Mechatronics*, vol. 21, pp. 1003-1012, 2011.

[7] S. J. Schroeck, W. C. Messner, and R. J. McNab, "On compensator design for linear time-invariant dual-input single-output systems," *IEEE/ASME Trans. Mechatron.*, vol. 6, no. 1, pp. 50-57, Mar. 2001.

[8] G. Herrmann, M. C. Turner, I. Postlethwaite, and G. Guo, "Practical implementation of a novel anti-windup scheme in a HDD-dual-stage servo system," *IEEE/ASME Trans. Mechatron.*, vol. 9, no. 3, pp. 580-592, Sep. 2004.

[9] T. Shen and M. Fu, "High precision and feedback control design for dual-actuator systems," in *Proc. IEEE Conf. Control Applications*, 2005, pp. 956-961.

[10] D. Kim, K.-T. Nam, S. H. Ji, and S. M. Lee, "Modeling of a dual actuator system and its control algorithm preventing saturation of fine actuator," in *Proc. IEEE/ASME Int. Conf. Advanced Intelligent Mechatronics*, 2011, pp. 530-535.

[11] G. Whitesides and H. Love, "The art of building small," *Scientif. Amer.*, vol. 285, no. 3, pp. 39-47, Sep. 2001.

[12] J. Yi, S. Chang, and T. Shen, "Disturbance-observer-based hysteresis compensation for piezoelectric actuators," *IEEE/ASME Trans. Mechatron.*, vol. 14, no. 4, pp. 456-464, Aug. 2009.

[13] D. Abramovitch, S. Andersson, L. Pao, and G. Schitter, "A tutorial on the mechanisms, dynamics, and control of atomic force microscopes," in *Proc. Amer. Control Conf.*, 2007, pp. 3488-2208.

[14] A. Fleming, "Nanopositioning system with force feedback for high-performance tracking and vibration control," *IEEE/ASME Trans. Mechatron.*, vol. 15, no. 3, pp. 433-447, Jun. 2010.

[15] M. Kobayashi, and R. Horowitz, "Track seek control for hard disk dual-stage servo systems," *IEEE Trans. Magn.*, vol. 37, no. 2, pp. 949-954, Mar. 2001.

[16] J. Zheng and M. Fu, "Nonlinear feedback control of a dual-stage actuator system for reduced settling time," *IEEE Trans. Contr. Syst. Technol.*, vol. 16, no. 4, pp. 717-725, Jul. 2008.

[17] K. Takaba, "A tutorial on preview control systems," in *Proc. SICE Annual Conference*, 2003, pp. 1388-1393.

[18] G. F. Franklin, J. D. Powell, and M. Workman, *Digital Control of Dynamic Systems*, 3rd ed., Addison Wesley Longman, 1997.